

Simultaneous Time-Resolved Measurements of Reflected Laser Power, Emittance and Radiance Temperature in Laser Powder Bed Fusion

David C. Deisenroth¹, Leonard Hanssen¹, Steven Grantham¹, Vladimir Khromchenko¹, and Sergey Mekhontsev¹

¹National Institute of Standards and Technology

Gaithersburg, MD, USA

Corresponding e-mail address: hanssen@nist.gov

Currently at NIST there is a significant effort aimed at establishing accurate metrology for the additive manufacturing processes. The purpose of our efforts include generation of reference data sets which could be used to validate multi-physics models. The measurands for comparison with multi-physics models include reflected process laser power, sample reflectance (emittance), and radiance temperature. Reflected power and sample reflectance are measured simultaneously with an integrating hemisphere that includes necessary gas flow provisions. Radiance temperature is measured with classical thermography.

INTRODUCTION

The Additive Manufacturing Metrology Testbed (AMMT) was commissioned in 2017 with a specific goal of supporting laser-based process of layerwise selective melting of the metallic powders [1]–[3].

This process is characterized by the heating laser typically operating at 1070 nm at power levels from 80 to several hundred watts, with spot sizes in the 65 to 120 micron range ($D4\sigma$, representing diameter within which about 95% of the Gaussian laser power profile is contained) and moving at a speed about 1 m/s. The process is defined by a combination of high-power density (on the order of 1 MW/cm²) and laser dwell time of about 100 μ s, resulting in very high spatial and temporal temperature gradients and complex thermo-fluid processes [4]–[6].

The experiments reported here were performed in the National Institute of Standards and Technology (NIST) Additive Manufacturing Metrology Testbed (AMMT). The AMMT is a custom LPBF research platform that was designed to be highly configurable for measurement of all aspects of the LPBF process. The AMMT includes a removable carriage that contains the build-well and a large metrology-well, both of which may be moved laterally within the large build chamber. The laser is an Yb-doped fiber laser with emission wavelength of 1070 nm. Laser power

delivery can be adjusted from 20 W to more than 400 W, with a 4-sigma diameter ($D4\sigma$, representing diameter within which about 95% of the Gaussian laser power profile is contained) spot size that is adjustable from 45 μ m to more than 200 μ m. The laser spot can be scanned with full control of the laser scan path/strategy at 100 kHz and laser power control at 50 kHz, with scan velocity from 0 mm/s to more than 4000 mm/s.

Due to fast growth of these technologies, significant efforts are underway nationwide to perform multi-physics simulation of the process, with an ultimate goal of achieving better understanding and improving production quality and speed [7], [8]. To simplify the task, it is common to start with a single track on a bare metal plate, then proceed with a multiline pad, and then add powder and proceed with a multi-layer builds, as each of these steps bring significant additional complexities.

METROLOGICAL GOALS

The purpose of our efforts include generation of reference data sets, which could be used to validate multi-physics models, which typically have to use multiple assumptions in order to keep the computing requirements within reasonable limits (as even the exascale computers struggle to cope with the first principle models) [9].

Signatures of interest of this process include time-resolved reflected laser power (frequently referred to as ‘laser coupling’), as well as spatially resolved temperature distribution in the process zone. Earlier reported independent efforts resulted in a well-documented laser power reflectometry [10], as well as radiance temperature [11] and reflectance [1] measurement capabilities. This research effort is aimed at prototyping an apparatus for simultaneous, dynamic (time-resolved) measurement of all three process signatures, namely (1) reflected process laser power (@1070 nm, not spatially resolved, directional-hemispherical geometry), (2) sample reflectance (@808 nm, spatially resolved,

hemispherical-directional geometry), and (3) sample radiance temperature (@850 nm, spatially resolved).

The schematic of the apparatus is shown in Fig. 1. The intention of measurements of emissivity and radiance temperature is of course to be able to generate true temperature distribution across the area of interest, but discussion of uncertainty of the true temperature is beyond the scope of this paper.

As shown in Fig. 1, the integrated reflected laser power is detected by radiometers with sintered polytetrafluoroethylene (PTFE) diffusers and a 1070 nm bandpass filters. The radiometers are calibrated by directing the (defocused) heating laser onto a reflectance standard in place of the sample. This is the directional-hemispherical reflectometer operation.

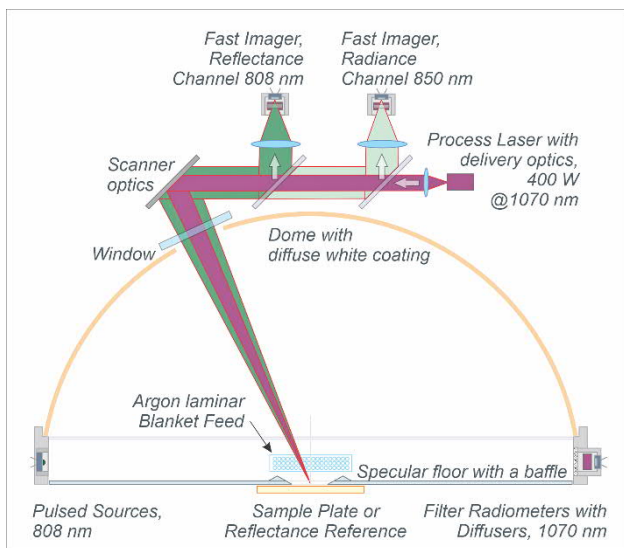


Fig. 1: Schematic of the experimental apparatus

For measurement of emittance, the reflectometer is operated in the hemispherical-directional mode. The probing light is provided by pulsed laser diodes at 808 nm. The narrow waveband of probing light is reflected from the sample and focused into the optics coaxially aligned with the heating laser. The first coaxial beam splitter provides an image of the narrow waveband of the reflected probing light of the laser-metal interaction scene that is then converted to emittance of the scene. A second coaxial beam splitter detects self-emitted light in a narrow waveband about 850 nm, which is then converted to NIST-traceable radiance temperature.

REFERENCES

1. S. Grantham, B. Lane, J. Neira, S. Mekhontsev, M. Vlasea, and L. Hanssen, Optical design and initial

2. B. Lane et al., Design, developments, and results from the NIST additive manufacturing metrology testbed (AMMT), in Solid Freeform Fabrication Symposium, Austin, TX, 1145–1160, 2016.
3. H. Yeung, J. Neira, B. Lane, J. Fox, and F. Lopez, Laser path planning and power control strategies for powder bed fusion systems, in The Solid Freeform Fabrication Symposium, 113–127, 2016.
4. Bidare, I. Bitharas, R. M. Ward, M. M. Attallah, and A. J. Moore, Fluid and particle dynamics in laser powder bed fusion, *Acta Materialia*, 142, 107–120, 2018.
5. A. Keshavarzkermani et al., An investigation into the effect of process parameters on melt pool geometry, cell spacing, and grain refinement during laser powder bed fusion, *Optics & Laser Technology*, 116, 83–91, 2019.
6. S. Ghosh et al., Single-track melt-pool measurements and microstructures in Inconel 625, *JOM*, 70(6), 1011–1016, 2018.
7. S. A. Khairallah, A. T. Anderson, A. Rubenchik, and W. E. King, Laser powder-bed fusion additive manufacturing: Physics of complex melt flow and formation mechanisms of pores, spatter, and denudation zones, *Acta Materialia*, 108, 36–45, 2016.
8. L. Levine, M. Stoudt, and B. Lane, A Preview of the NIST/TMS Additive Manufacturing Benchmark Test and Conference Series, *JOM* (1989), 70, 2018.
9. M. Mozaffar, E. Ndip-Agbor, S. Lin, G. J. Wagner, K. Ehmman, and J. Cao, Acceleration strategies for explicit finite element analysis of metal powder-based additive manufacturing processes using graphical processing units, *Computational Mechanics*, 64(3), 879–894, 2019.
10. D. C. Deisenroth, S. Mekhontsev, and B. Lane, Measurement of mass loss, absorbed energy, and time-resolved reflected power for laser powder bed fusion, in SPIE Photonics West, San Francisco, 2020.
11. I. Zhirnov, S. Mekhontsev, B. Lane, S. Grantham, and N. Bura, Accurate determination of laser spot position during laser powder bed fusion process thermography, *Manufacturing Letters*, 23, 49–52, 2020.